

Electrochemistry Cell Model

Dennis Dees and Kevin Gallagher
Chemical Sciences and Engineering Division

May 9-13, 2011

Vehicle Technologies Program Annual Merit Review and
Peer Evaluation Meeting
Washington, D.C.

Project ID:
ES031

This presentation does not contain any proprietary,
confidential, or otherwise restricted information.

Overview

Timeline

- Start: October 2008
- Finish: September 2014
- ~43% Complete

Budget

- Total project funding
 - 100% DOE
- FY2010: \$400K
- FY2011: \$400K

Barriers

- Development of a safe cost-effective PHEV battery with a 40 mile all electric range that meets or exceeds all performance goals
 - Interpreting complex cell electrochemical phenomena
 - Identification of cell degradation mechanisms

Partners (Collaborators)

- Daniel Abraham, Argonne
- Sun-Ho Kang, Argonne
- Andrew Jansen, Argonne
- Wenquan Lu, Argonne
- Kevin Gering, INL

Objectives, Milestones, and Approach

- The objective of this work is to correlate analytical diagnostic results with the electrochemical performance of advanced lithium-ion battery technologies for PHEV applications
 - Link experimental efforts through electrochemical modeling studies
 - Identify performance limitations and aging mechanisms
- Milestones for this year:
 - Initiate development of AC impedance two phase model (completed)
 - Integrate SEI growth model into full cell model (completed)
- Approach for electrochemical modeling activities is to build on earlier successful characterization and modeling studies in extending efforts to new PHEV technologies
 - Expand and improve data base and modeling capabilities

Major Accomplishments and Technical Progress

- Adopted new differential equation solver software (PSE gPROMS) to address several long term issues limiting model advancement
 - Integrating complex dynamic interfaces into full cell Li-ion models to examine factors limiting performance and life
 - Streamlining parameter estimation for new cell chemistries
 - Implementing the AC impedance version of model with increasingly more intricate interfacial and bulk active particle phenomena
- Implemented SEI growth model on the negative electrode to analyze capacity fade mechanisms including cross-interactions with positive electrode
- Developed 3D electrochemical model to examine primary-secondary active particle microstructure and properties affecting impedance (e.g. porosity, surface area, electronic conductivity, electronic contacts, and electrolyte wetting)
- Utilized electrochemical model to further examine electrode thickness limitations

Description of Electrochemical Model

- Phenomenological model developed for AC impedance and DC studies using same constituent equations and parameters
- Combines thermodynamic, kinetic, and interfacial effects with continuum based transport equations
- Complex active material / electrolyte interfacial structure
 - Film on active particles acts as an electrolyte layer with restricted diffusion and migration of lithium ions
 - Surface layer of active particle inhibits the diffusion of lithium into the bulk active material
 - Electrochemical reaction and double layer capacitance at film/layer interface
 - Particle contact resistance and film capacitance
- Volume averaged transport equations account for the composite electrode geometry
- Lithium diffusion and possible phase change in active particles included, along with multiple particle fractions
- The system of coupled differential equations are solved numerically
- Model parameters determined independently (e.g. electrolyte parameters are supplied by Kevin Gering's Advanced Electrolyte Model)



Increasingly Complex Electrochemical Cell Model Comprised of Dynamic Coupled One-Dimensional Multi-Scale Subsystems

Transport through Cell Sandwich

$$\varepsilon \frac{\partial c}{\partial t} = \frac{\varepsilon}{\tau} \frac{\partial}{\partial x} \left(D \frac{\partial c}{\partial x} \right) + \frac{1}{z_+ v_+ F} \frac{\partial \left[(1 - c \bar{V}_e) (1 - t_+^o) i_2 \right]}{\partial x}$$

$$i_2 = -\frac{\kappa \varepsilon}{\tau} \frac{\partial \Phi_2}{\partial x} - v R T \frac{\kappa \varepsilon}{F \tau} \left(\frac{s_+}{n v_+} + \frac{t_+^o}{z_+ v_+} \right) \left(1 + \frac{\partial \ln f_{\pm}}{\partial \ln c} \right) \frac{1}{c} \frac{\partial c}{\partial x}$$

$$\frac{\partial i_2}{\partial x} = F z_+ \sum_k a_k j_{kn} \quad I = i_1 + i_2 \quad i_1 = -\sigma_{eff} \frac{\partial \Phi_1}{\partial x}$$

Bulk Solid-State Phase Transition & Diffusion

$$\frac{\partial (\varepsilon_{S1} c_{S1} + \varepsilon_{S2} c_{S2} + \varepsilon_{S3} c_{S3})}{\partial t} = \frac{\partial}{\partial y} \left(\frac{\varepsilon_{S1} D_{S1}}{\tau_{S1}} \frac{\partial c_{S1}}{\partial y} + \frac{\varepsilon_{S2} D_{S2}}{\tau_{S2}} \frac{\partial c_{S2}}{\partial y} + \frac{\varepsilon_{S3} D_{S3}}{\tau_{S3}} \frac{\partial c_{S3}}{\partial y} \right)$$

$$\frac{\partial \varepsilon_{S2}}{\partial t} = K_{S12} \varepsilon_{S1} - K_{S21} \varepsilon_{S2} + K_{S32} \varepsilon_{S3} - K_{S23} \varepsilon_{S2}$$

$$\frac{\partial \varepsilon_{S3}}{\partial t} = K_{S23} \varepsilon_{S2} - K_{S32} \varepsilon_{S3}$$

- Adopted new differential algebraic equation solver package (PSE gPROMS®) that will solve a wide variety of cell studies at the required level of complexity

Bulk Solid-State Diffusion

$$\frac{\partial c_{sb}}{\partial t} = \frac{\partial}{\partial z} \left(D_{sb} \frac{\partial c_{sb}}{\partial z} \right)$$

Negative SEI Reaction/Transport

$$\frac{\partial c_f}{\partial t} - \frac{y}{L_f} \frac{\partial L_f}{\partial t} \frac{\partial c_f}{\partial Y} = \frac{D_f}{(L_f)^2} \frac{\partial^2 c_f}{\partial Y^2} \quad -i_{2,f} = \frac{z_+ v_+ F}{L_f} \left[(z_+ u_+ - z_- u_-) F c_f \frac{\partial \Phi_{2,f}}{\partial Y} + (D_+ - D_-) \frac{\partial c_f}{\partial Y} \right]$$

$$\frac{\partial i_{2,f}}{\partial y} = 0 \quad \frac{dL_f}{dt} = v_f = \frac{-j_{n2}}{c_{SEI}} \quad i_n = F \sum z_i j_{n,i}$$

$$j_{n1} = k_1^0 \left\{ c_{s,k} e^{\frac{\alpha_1 F (\Phi_1 - \Phi_f)}{RT}} - K_1 c_{+,f} (c_T - c_{s,k}) e^{\frac{-\alpha_1 F (\Phi_1 - \Phi_f)}{RT}} \right\} \quad j_{n2} = k_2^0 \left\{ c_f e^{\frac{\alpha_2 F (\Phi_1 - \Phi_f)}{RT}} - K_2 e^{\frac{-\alpha_2 F (\Phi_1 - \Phi_f)}{RT}} \right\}$$

$$j_{n1} = k_1^0 \left\{ c_{+,f} e^{\frac{\alpha_1 F (\Phi_f - \Phi_2)}{RT}} - K_1 c e^{\frac{-\alpha_1 F (\Phi_f - \Phi_2)}{RT}} \right\} \quad j_{n2} = -k_2^0 c_{-,f} c_{+,f} e^{\frac{-\alpha_2 F (\Phi_f - \Phi_2 - U_2)}{RT}}$$

Positive SEI Reaction/Transport

$$\frac{\partial c_+}{\partial t} = D_+ \left(\frac{\partial^2 c_+}{\partial y^2} \right) \quad \eta_f = \frac{i_n \delta_f}{\kappa_f} + \frac{RT s_+}{nF} \ln \frac{c_+ |_{electrolyte}}{c_+ |_{lactive material}}$$

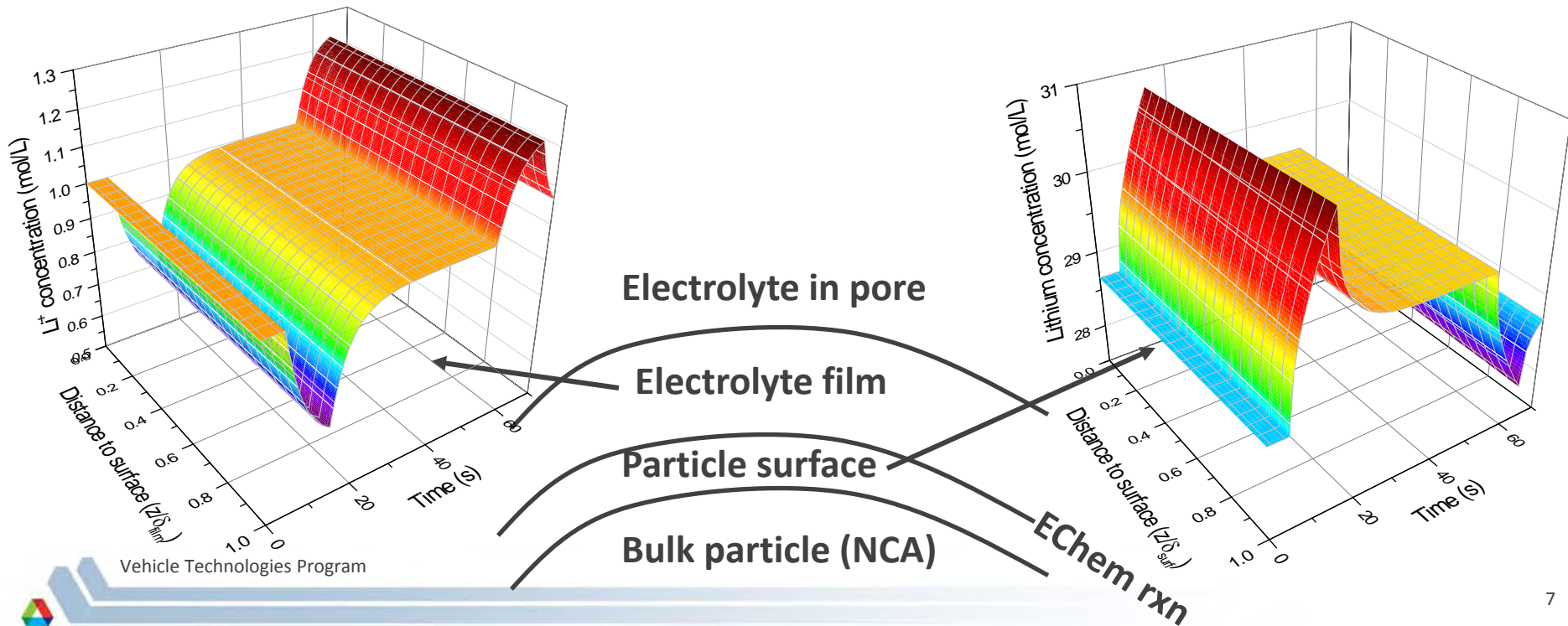
$$\frac{\partial c_{Si}}{\partial t} = D_{Si} \left(\frac{\partial^2 c_{Si}}{\partial y^2} \right)$$

$$i_n = i_0 \left(\frac{c_+}{c_{+,ref}} \right)^{\alpha_A} \left(\frac{c_{Ti} - c_{Si}}{c_{Ti} - c_{Si,ref}} \right)^{\alpha_A} \left(\frac{c_{Si}}{c_{Si,ref}} \right)^{\alpha_C} \left\{ e^{\left[\frac{\alpha_A F \eta_K}{RT} \right]} - e^{\left[\frac{-\alpha_C F \eta_K}{RT} \right]} \right\}$$

$$\eta_R = \sigma_p z_+ F j_n$$

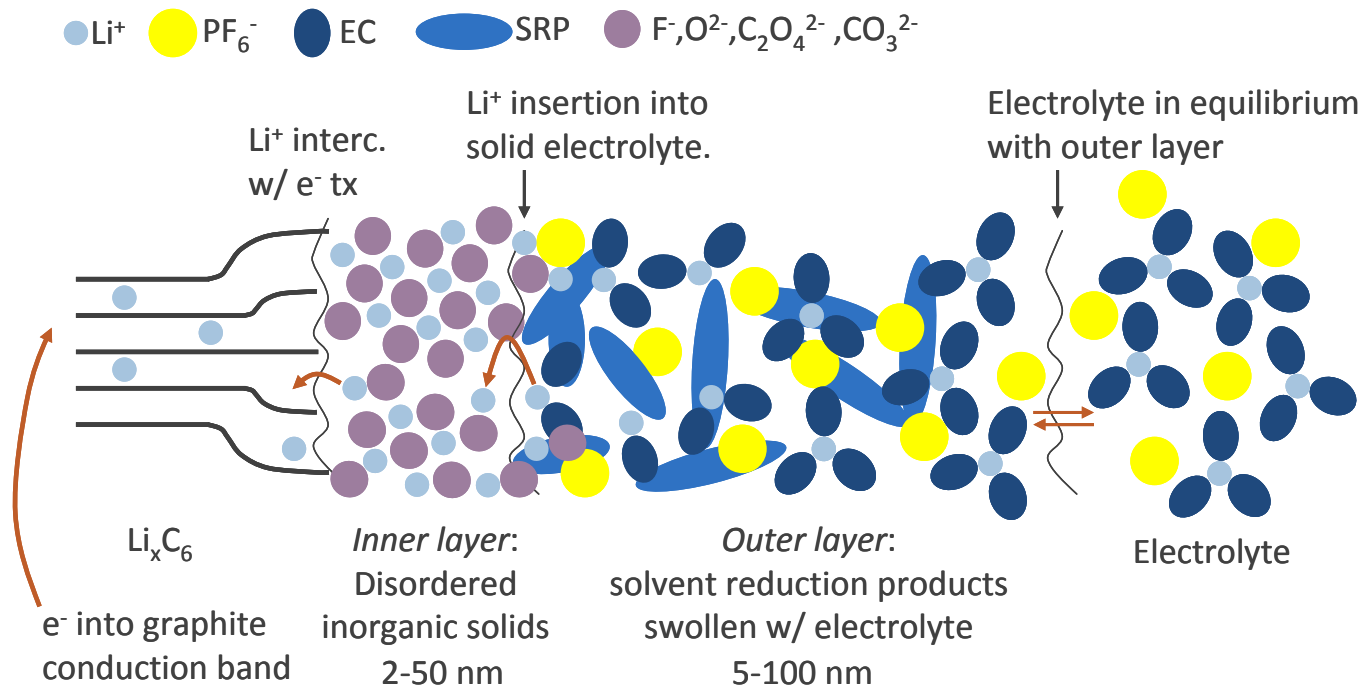
Advantages & Current Status of Software Implementation

- Previously treated coupled multi-scale problems using a multi-dimensional solver
- New approach explicitly treats each length scale to allow for greater stability and increased dynamic complexity
- Successfully recreated past DC modeling work with increased complexity capable of examining short time scales
 - Dynamic multi-layered interfaces on particles in porous electrode
 - Figures for a 15C/11.25C HPPC test with current relaxation at end



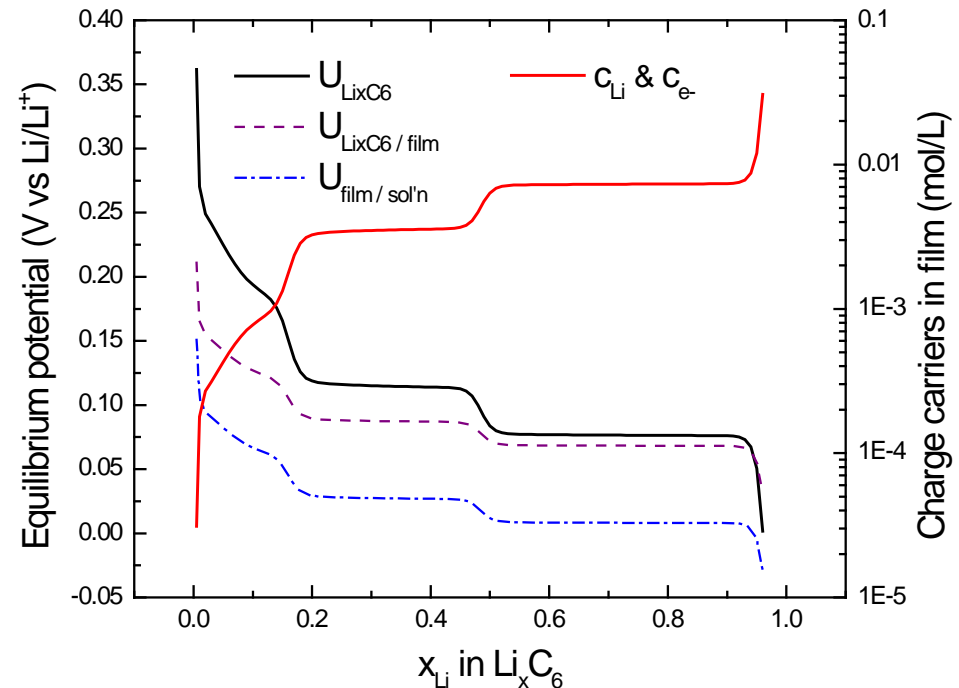
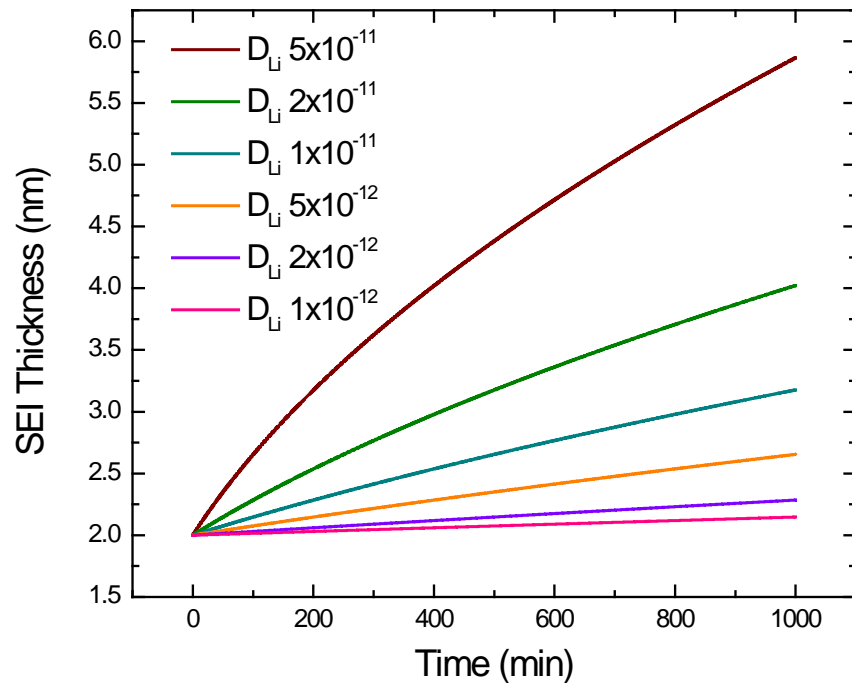
SEI Growth Model Implementation

- Implementing SEI growth model necessary to understand power and energy fade of future cell builds
- Differing negative electrode aging behavior from Gen 2 to Gen 3
 - Graphite changed from MAG10 to MCMB
 - Positive electrode changed from NCA to NCM
 - Gen 2 negative impedance stabilized; Gen 3 continuously increased



SEI Growth Model Status

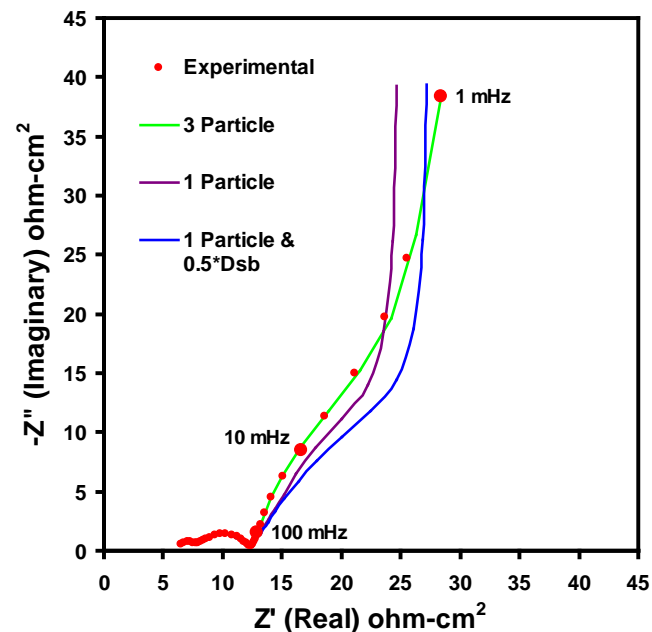
- Single phase SEI growth model completed for single particle and implemented in porous electrode
 - Coupled Li interstitial and electron transport through insulating film¹
- Parameter estimation in progress for film transport properties



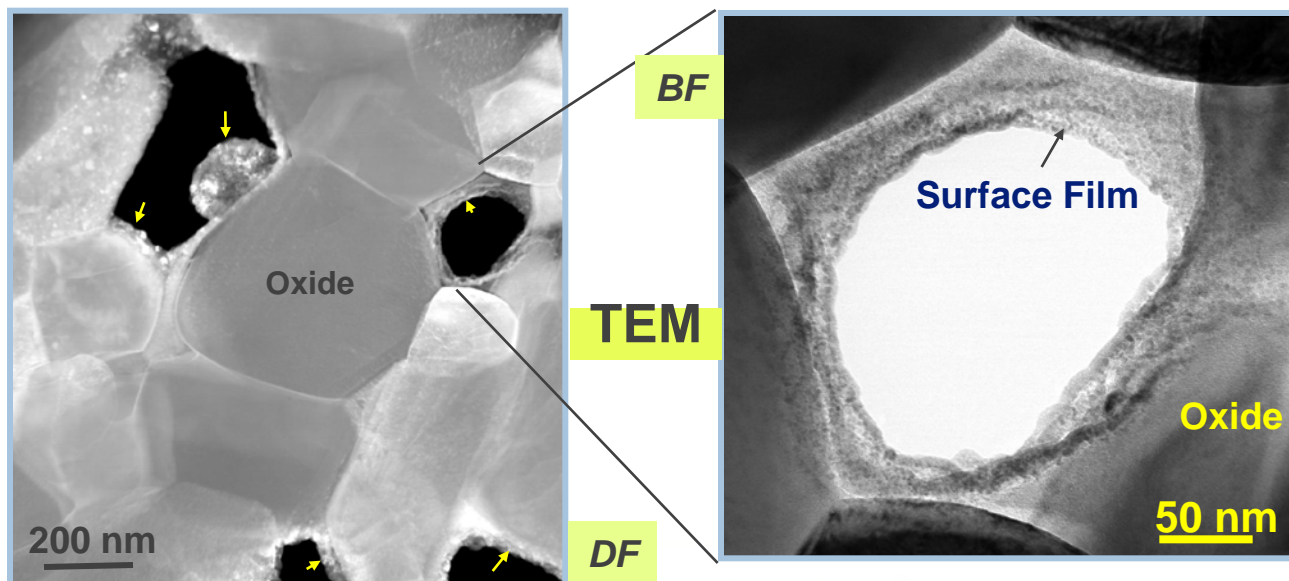
1. J. Christensen and J. Newman, *J. Electrochem. Soc.* **151** (11) A1977 (2004)

Primary-Secondary Positive Active Particle Microstructure

- Electron microscopy images of many positive active materials indicate the secondary particles have some degree of porosity
- NCA positive electrode low frequency Warburg EIS data could only be fit using multiple active material particle fractions
- Characteristic diffusion lengths from EIS studies indicate electrochemical reactions penetrate secondary oxide particles



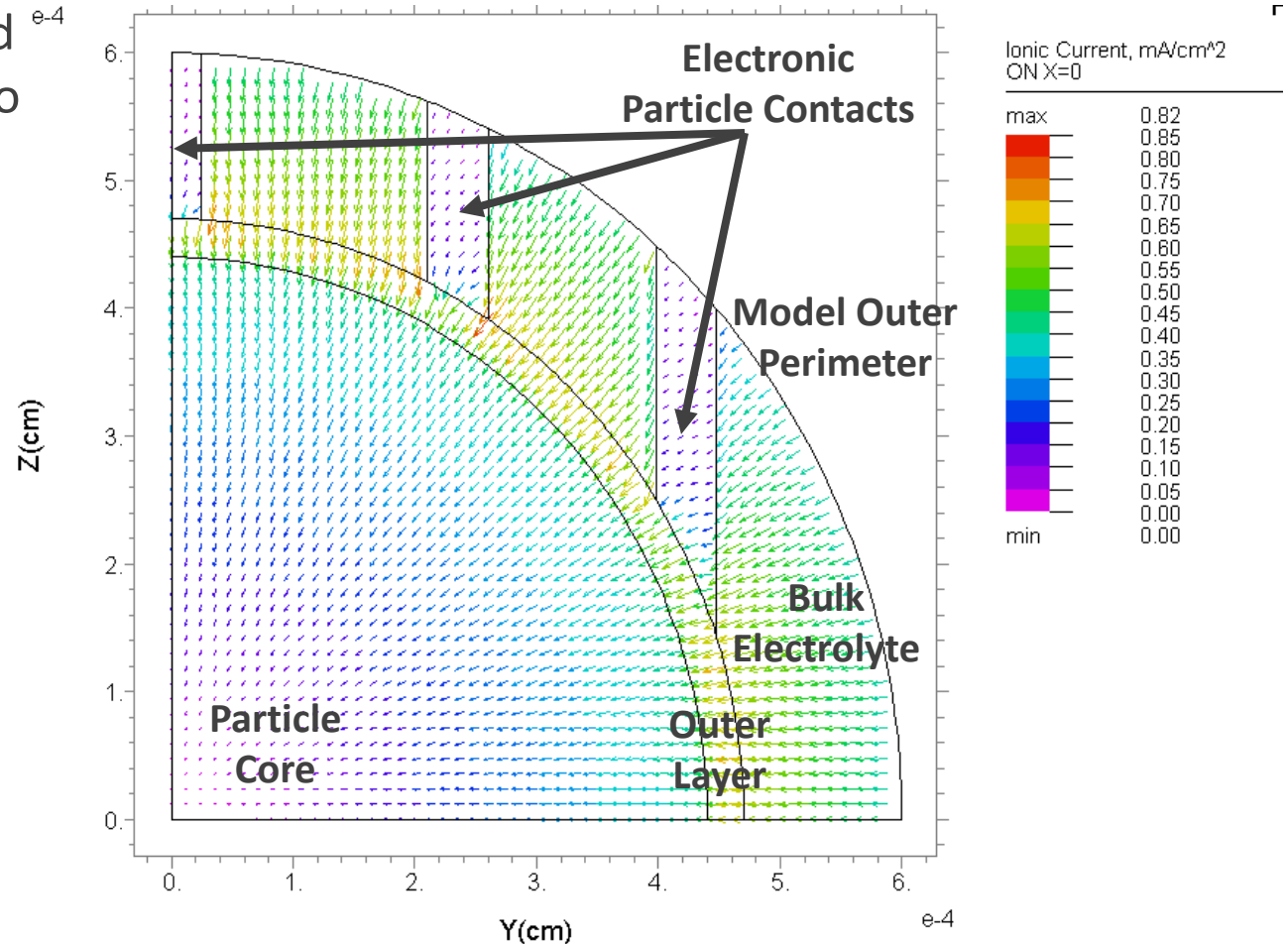
- TEM images of aged NCA particles show films on the surface of the secondary particles and in pores between primary particles



3D Electrochemical Model Developed for Positive Active Material Spherical Secondary Particle

- Electrochemical model with simplified SEI relation applied to particle scale
- Secondary particle assumed to be made of primary particles with independent core and outer layer characteristics
- Particle porosity allows access of electrolyte and ionic current to reach into the particle core

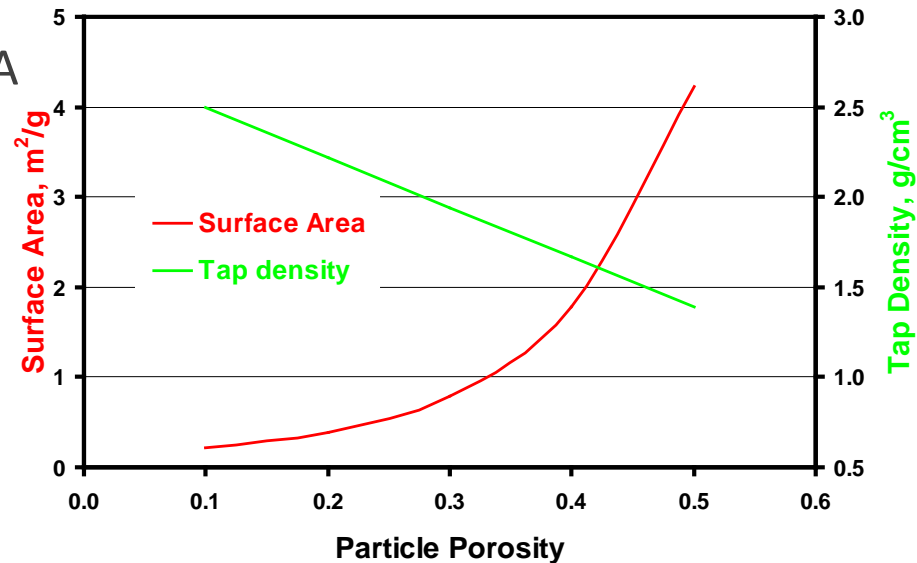
Ionic Current Distribution in Secondary Particle



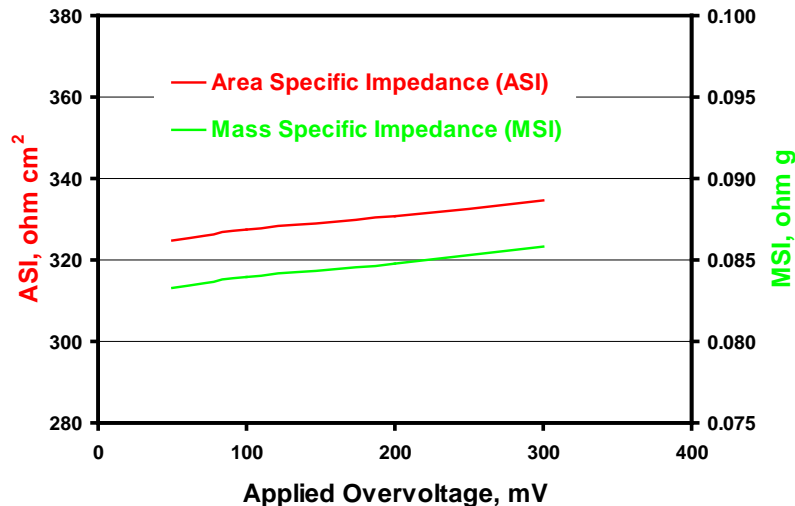
Particle Properties Established and Impedance Terms Defined to Assess Particle Performance

- Wealth of diagnostic studies and associated model development for NCA active material with Gen 2 electrolyte utilized to create baseline parameter set and particle characteristics
- Simple relations developed for active material surface area and tap density with changes in particle porosity

Estimated Change in Particle Characteristics



Particle Impedance, 10s Discharge Pulse

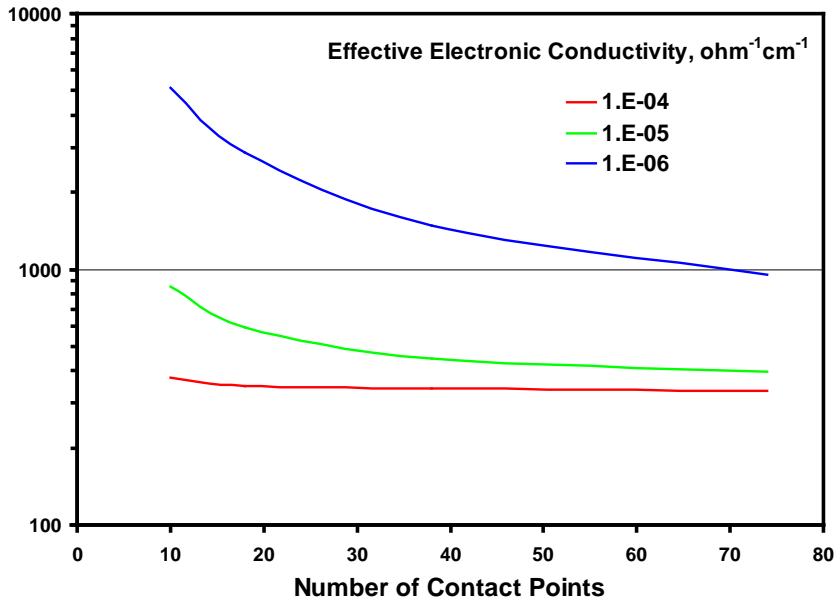


- Two specific impedance terms are used to describe particle performance: area (ASI), based on particle active area (i.e. not the electrode area), and particle mass (MSI)
- When the ratio of active area to mass is fixed then both impedance effects behave similarly, as is the case for the change in particle impedance with applied voltage

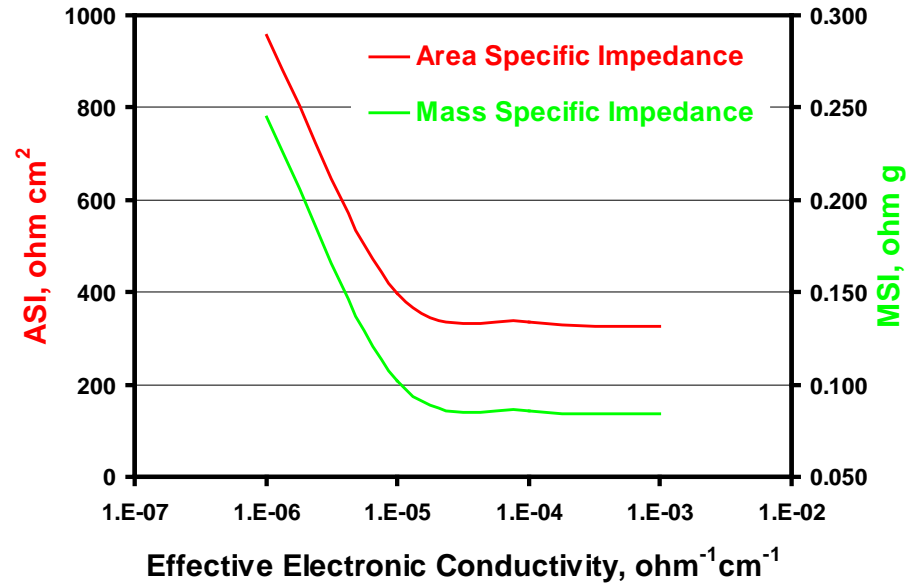
Impact of Electronic Conductivity on Particle Performance

- At effective electronic conductivities less than about $10^{-5} \Omega^{-1} \text{ cm}^{-1}$ the particle impedance is a strong function of conductivity
- The impedance is governed by other phenomena at greater conductivities

Particle Impedance, 10s Discharge Pulse
0.5 micron Contact Diameter



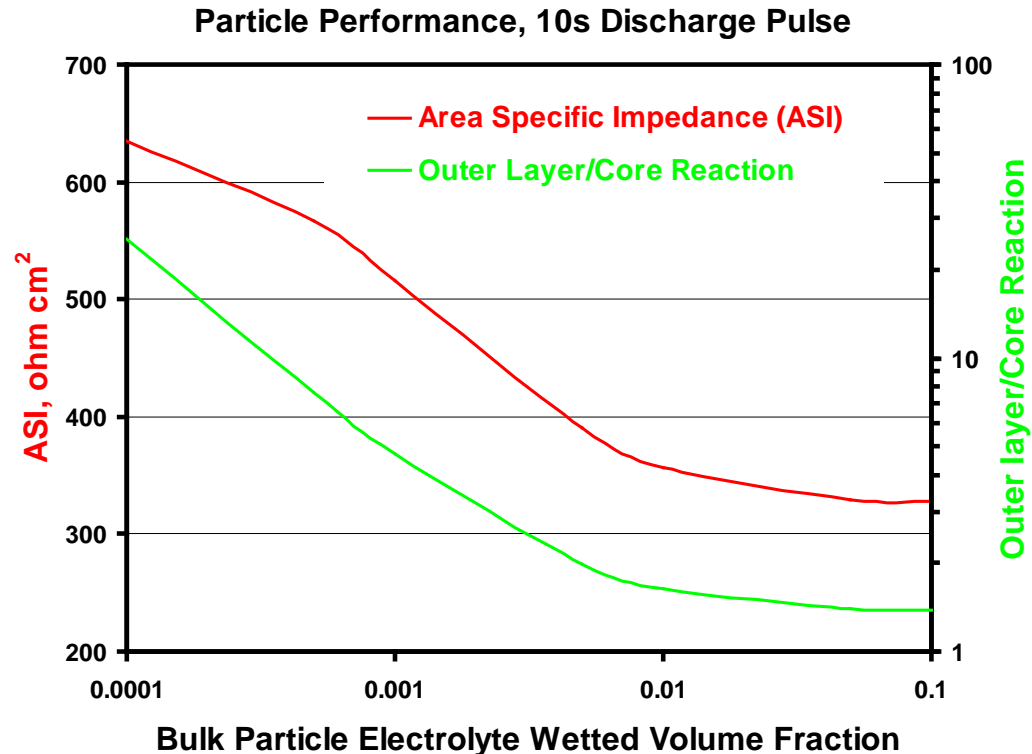
Particle Impedance, 10s Discharge Pulse



- The particle impedance is relatively independent of the number of contacts for effective electronic conductivities greater than $10^{-4} \Omega^{-1} \text{ cm}^{-1}$
- Varying the diameter of the particle contacts can have a similar impact on impedance

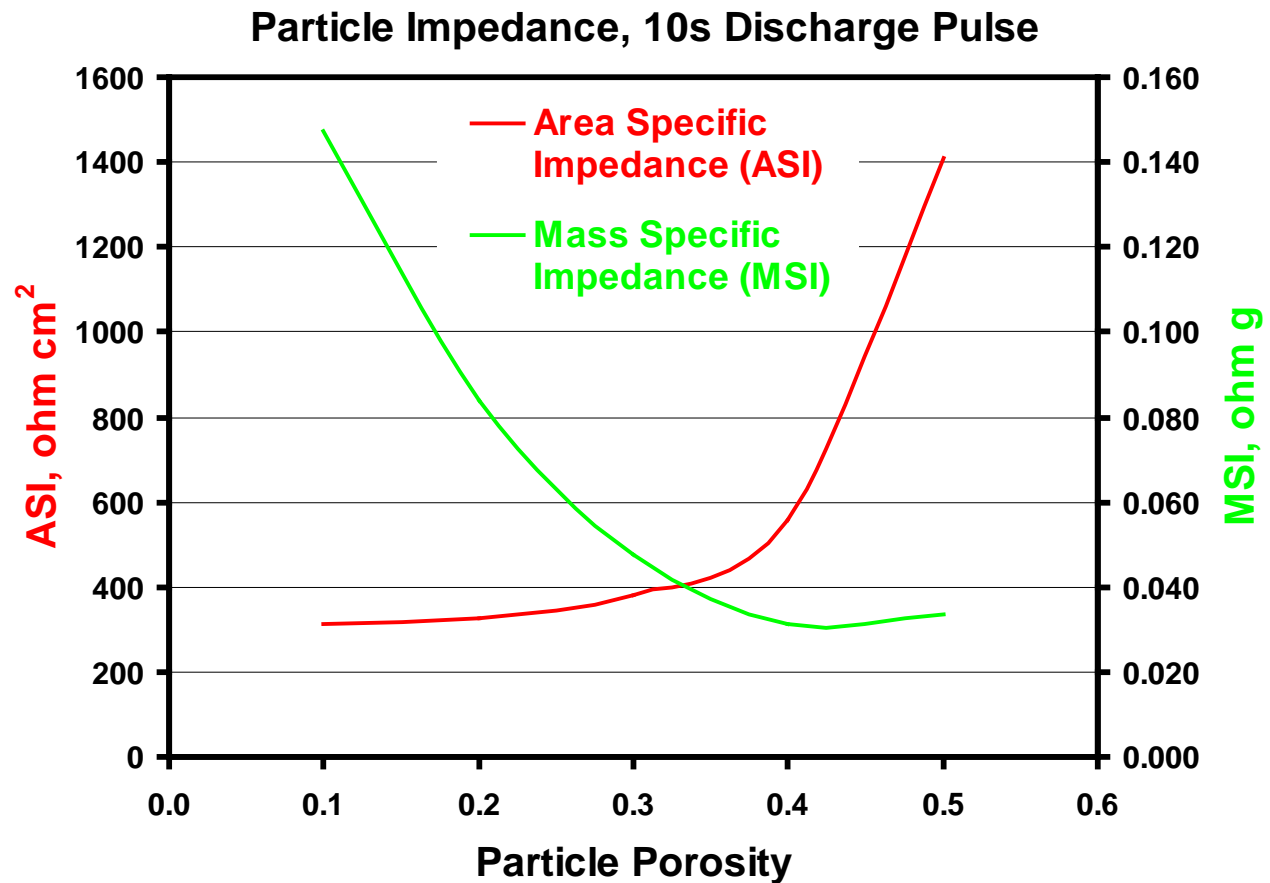
Electrolyte Soaking into Particle Significantly Improves Performance

- It is much easier for Li ions to diffuse through the liquid electrolyte than the the solid-state oxide active material by a factor of about 10^4
- Therefore, even a small amount of electrolyte in the oxide particle pores can enhance the overall electrochemical reaction in the core of the particle and reduce its impedance
- The impedance levels out at higher volume fractions because the electrochemical reaction in the core is not limited by Li ion transport in the electrolyte
- At lower volume fractions the amount of electrochemical reaction in the core goes to zero and the impedance is governed by the reaction in the outer layer



Impact of Particle Porosity on Particle Performance

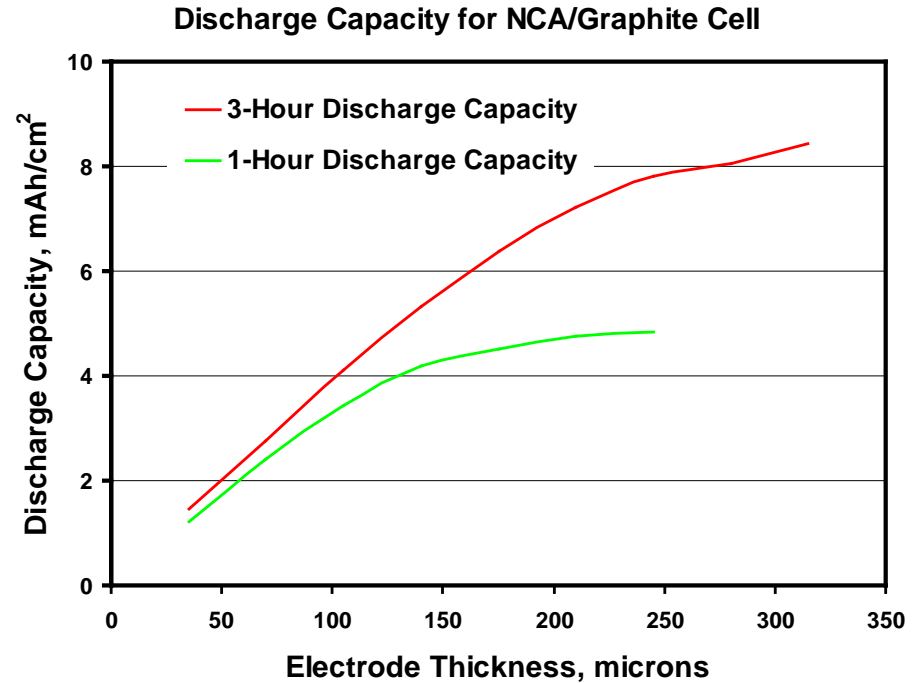
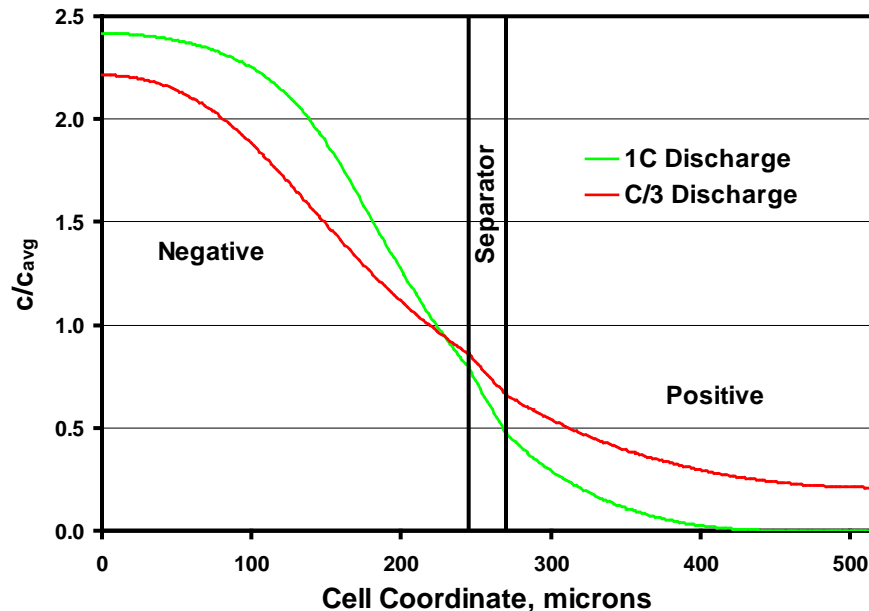
- As the particle porosity increases, its active surface area rises dramatically reducing the particle impedance on a gravimetric basis
- For a fixed applied polarization, the particle impedance on an active area basis rises significantly with increasing porosity
- As the porosity increases, there is less active material available for the lithium to diffuse into, resulting in increasingly higher concentration polarization and ASI



Electrochemical Model Utilized to Examine Electrode Thickness Limitations

- The cell discharge capacity effectively reaches a limiting capacity with increasing electrode thickness
- During discharge, salt concentration in positive approaches zero

Salt Concentration Distribution
NCA/Graphite Cell at End-of-Discharge
245 micron Electrodes

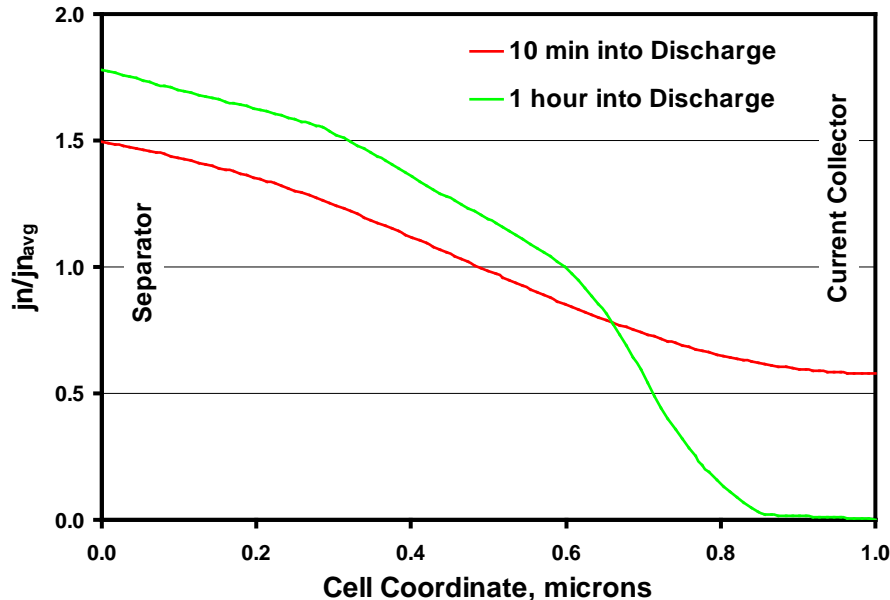


- Lowering the discharge current allows a greater fraction of the electrode capacity to be utilized
- As electrode thickness increases transport of salt in electrolyte limits constant C-rate discharge capacity

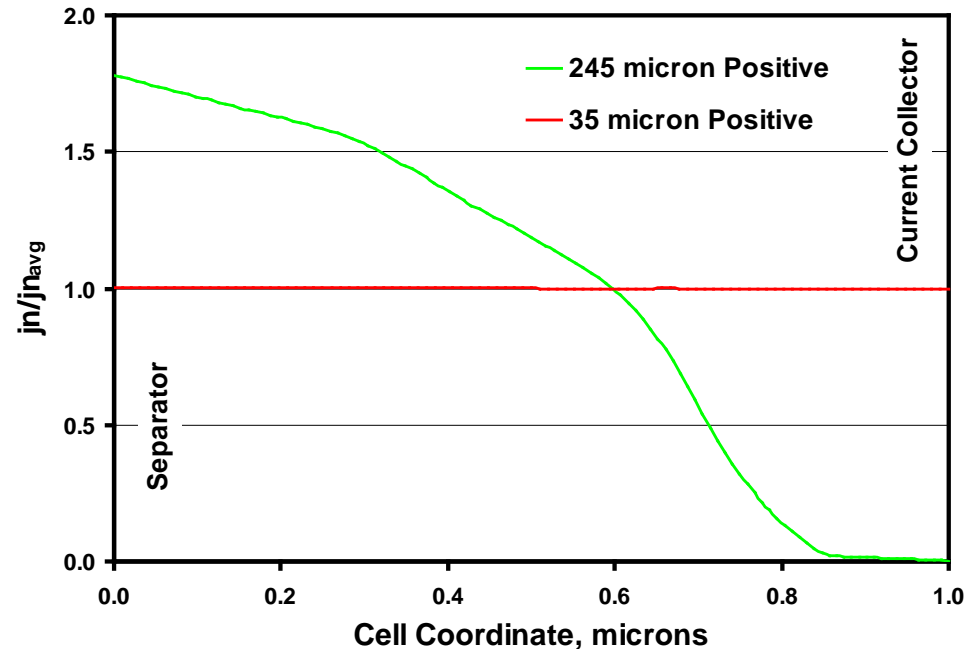
Increasing Electrode Thickness Affects the Current Distribution in Electrodes

- Because of a relatively large interfacial impedance, thinner electrodes (i.e. $\sim \leq 150 \mu\text{m}$ for 1C discharge) have a relatively uniform current distribution

Current Distribution in Positive Electrode
1C Discharge of NCA/Graphite Cell
245 micron Electrodes



Current Distribution in Positive Electrode
1C Discharge of NCA/Graphite Cell
One Hour into Discharge

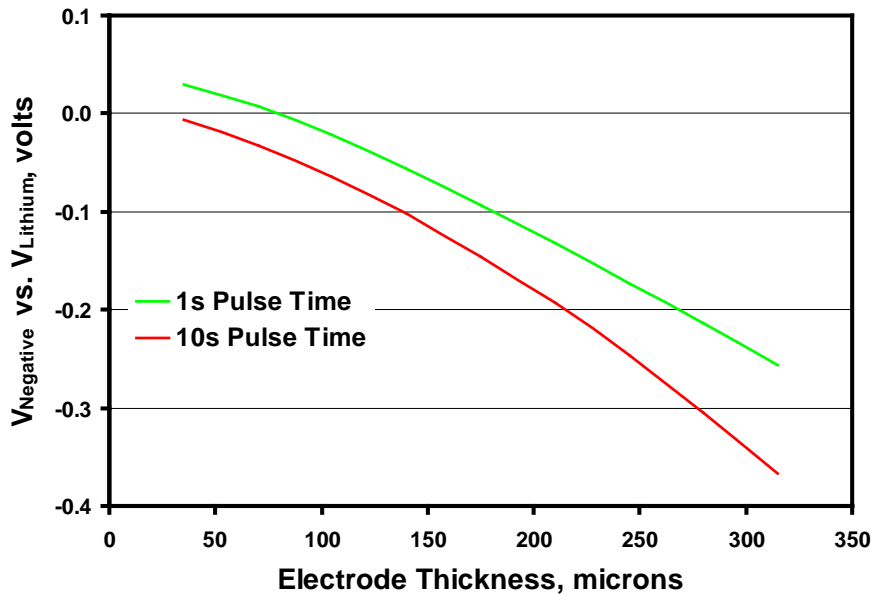


- Electrolyte transport limitations in thick electrodes shifts the current towards the separator that changes continuously during discharge

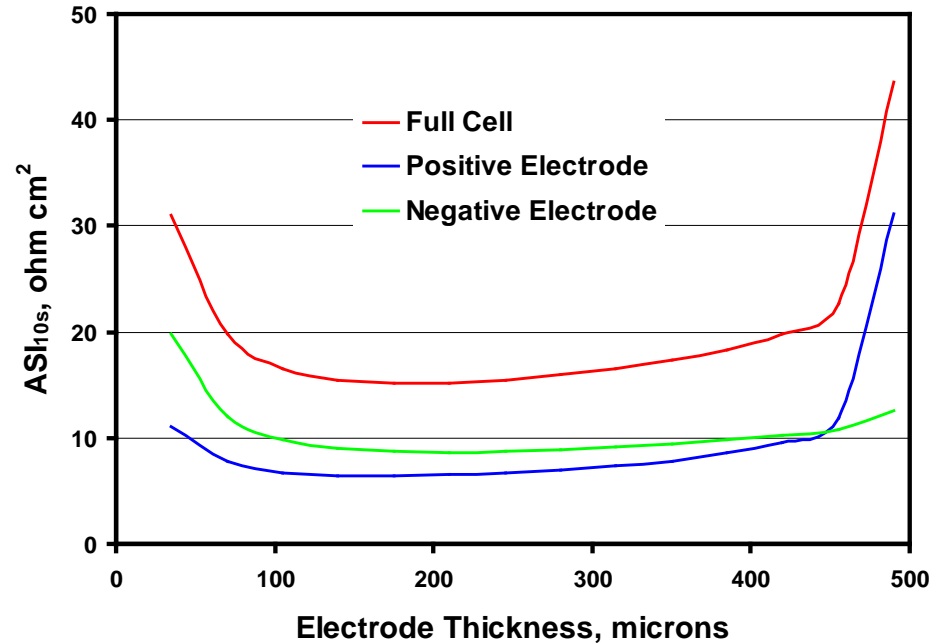
Electrode Impedance Relatively Constant Over a Wide Thickness Range

- Impedance of thin electrodes increase as the active area decreases
- Thick electrode cell impedance increases result from electrolyte transport limitations

5C Charge Pulse
NCA/Graphite Cell at 60%SOC



10 s 5C Discharge Pulse ASI
NCA/Graphite Cell at 60%SOC



- Primary performance limitation for thick electrodes is that thicker graphite negatives can dip below the lithium deposition voltage during regen charging pulses

Future Plans

- Advance development of PHEV focused electrochemical models using new differential algebraic equation solver package (PSE gPROMS)
 - Continue conversion of existing models
 - Develop full numerical AC impedance version
 - Utilize parameter fitting routines in new software to examine advanced PHEV couples
- Continue development electrochemical models directed towards examining capacity fade phenomena
 - Implement cation accelerated growth of SEI (e.g. Mn^{2+} , Li^+ , etc)
 - Implement dual layer SEI growth
 - Address cycle and calendar aging tests (large time scales)
- Continue support of other ABR projects
- Milestones for next year
 - Complete conversion of existing models
 - Complete implementation and initial testing of full SEI growth model
 - Initiate parameter estimation of high-energy NMC/graphite system

Summary

- The objective of this work is to correlate analytical diagnostic results with the electrochemical performance of advanced lithium-ion battery technologies for PHEV applications
- Approach for electrochemical modeling activities is to build on earlier successful characterization and modeling studies in extending efforts to new PHEV technologies
- Technical Accomplishments
 - Adopted new differential equation solver software
 - Implemented SEI growth model on the negative electrode to analyze capacity fade mechanisms
 - Developed 3D electrochemical model to examine primary-secondary active particle microstructure
 - Utilized electrochemical model to further examine electrode thickness limitations
- Future plans include the continued development of PHEV focused electrochemical models, further development of models examining capacity fade phenomena, and support of other ABR projects

Acknowledgment

Support for this work from DOE-EERE, Office of Vehicle Technologies is gratefully acknowledged

- David Howell**
- Peter Faguy**

